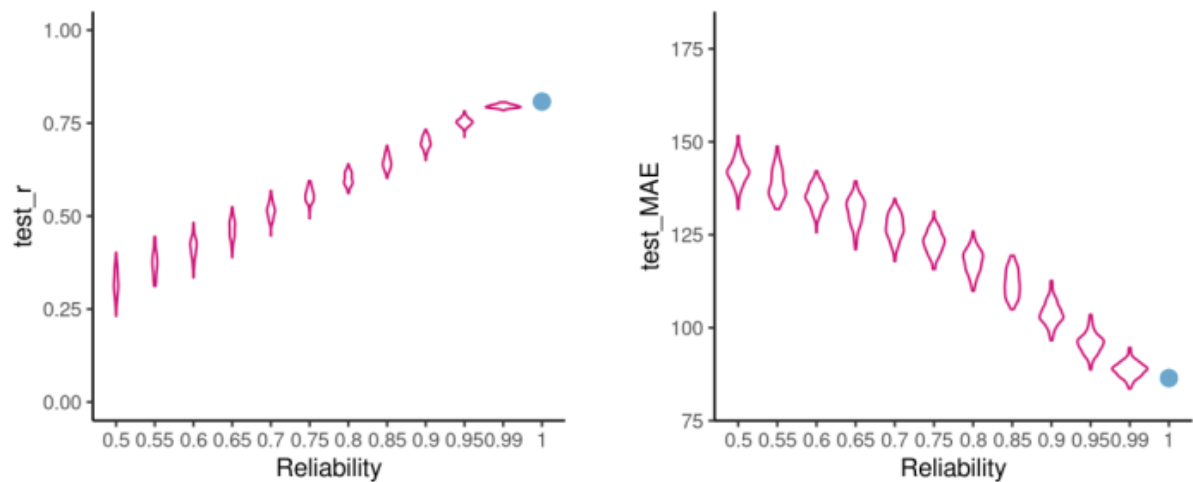


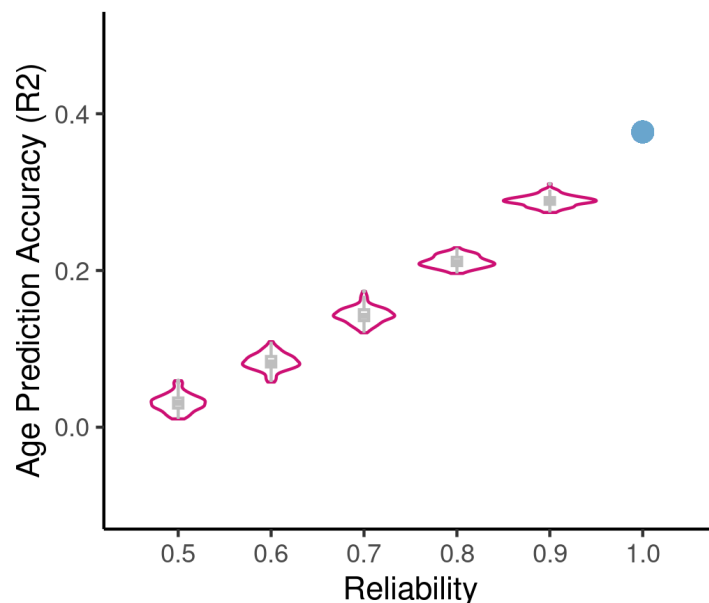
Supplementary Results

Prediction accuracy for age prediction - additional metrics



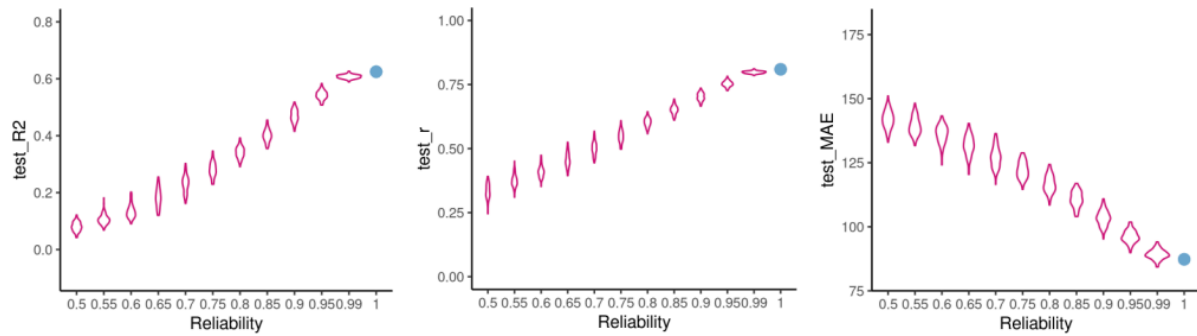
Supplementary Figure 1. Mean absolute error (MAE) and correlation between observed and predicted targets in age prediction. Each violin plot summarises the accuracy of predicting 100 simulated datasets within each reliability band.

Sensitivity analyses - Age prediction

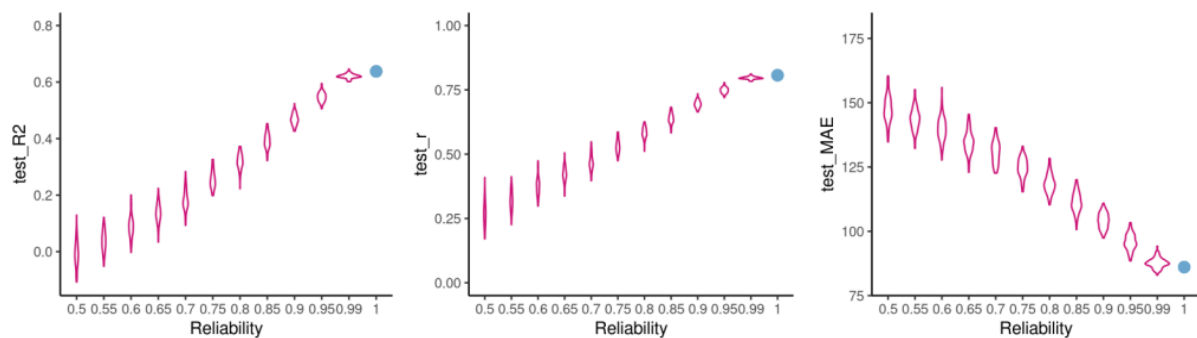


Supplementary Figure 2. Prediction of age using 5000 subjects from the UKB. The same sample of participants was used to create this figure as in the section "Behavioural reliability

is related to prediction accuracy” of the results. The age of subjects was predicted using ridge regression as in Figure 1 and accuracy was evaluated using R2. Each violin plot summarises the accuracy of predicting 100 simulated datasets within each reliability band. Boxplots are centred at the median, with the bounds representing the interquartile range, and whiskers the min/max values, outliers are not shown.

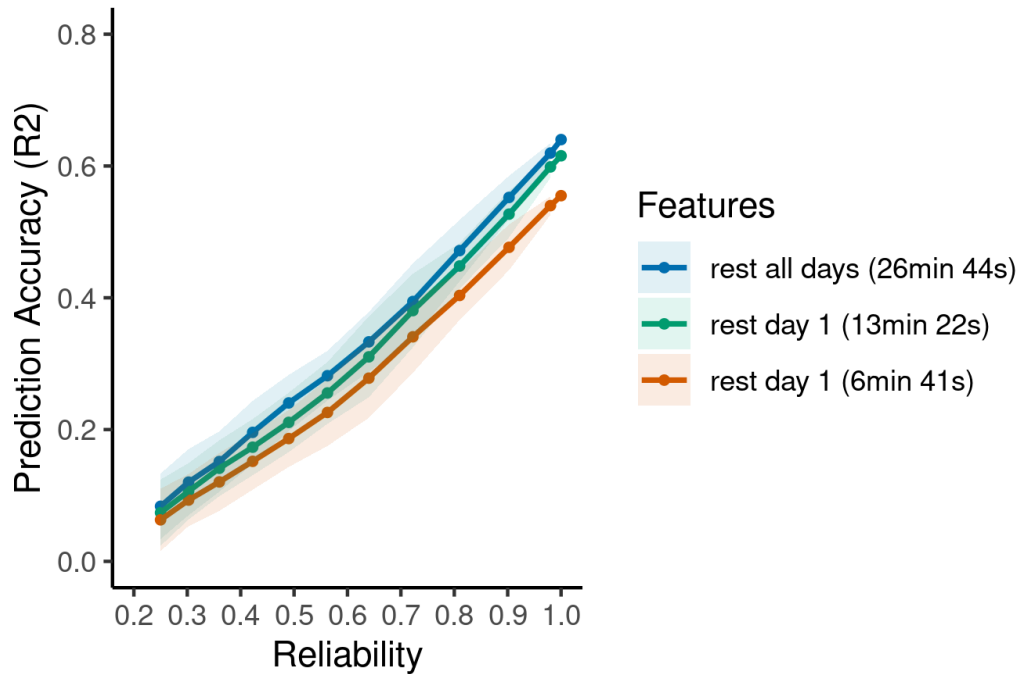


Supplementary Figure 3. Prediction Using Seitzman et al. (2020) Nodes. R2, Mean absolute error (MAE) and correlation between observed and predicted targets in age prediction using 300 nodes by Seitzmann et al. 2020. Each violin plot summarises the accuracy of predicting 100 simulated datasets within each reliability band.

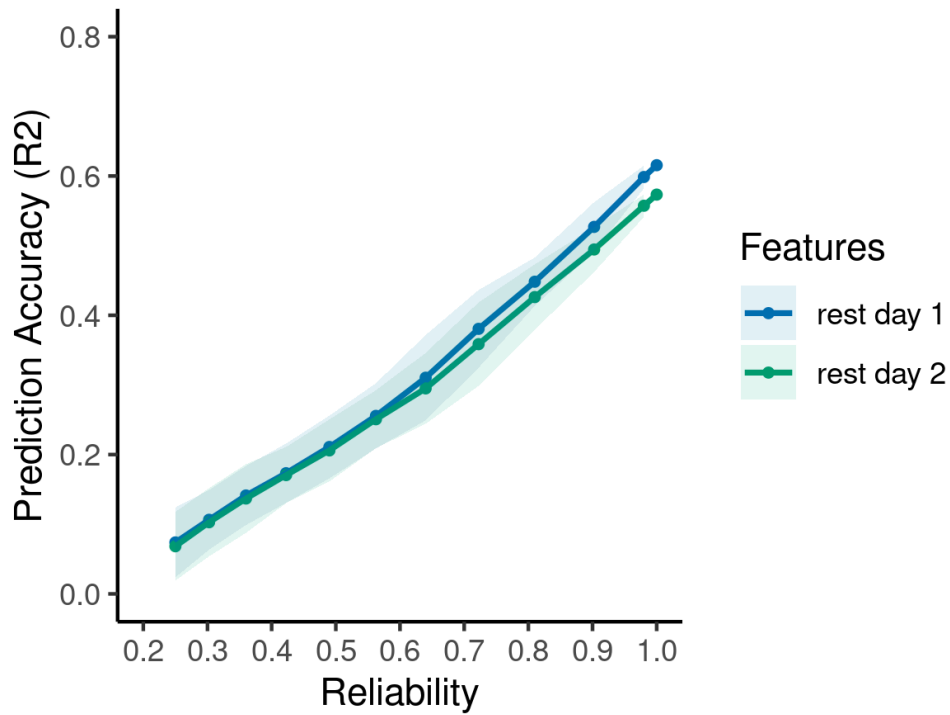


Supplementary Figure 4. Prediction Using Support Vector Regression. R2, Mean absolute error (MAE) and correlation between observed and predicted targets in replication of age prediction using support vector regression. Each violin plot summarises the accuracy of predicting 100 simulated datasets within each reliability band.

Impact of reliability on prediction accuracy in the HCP-A dataset - influence of connectivity reliability

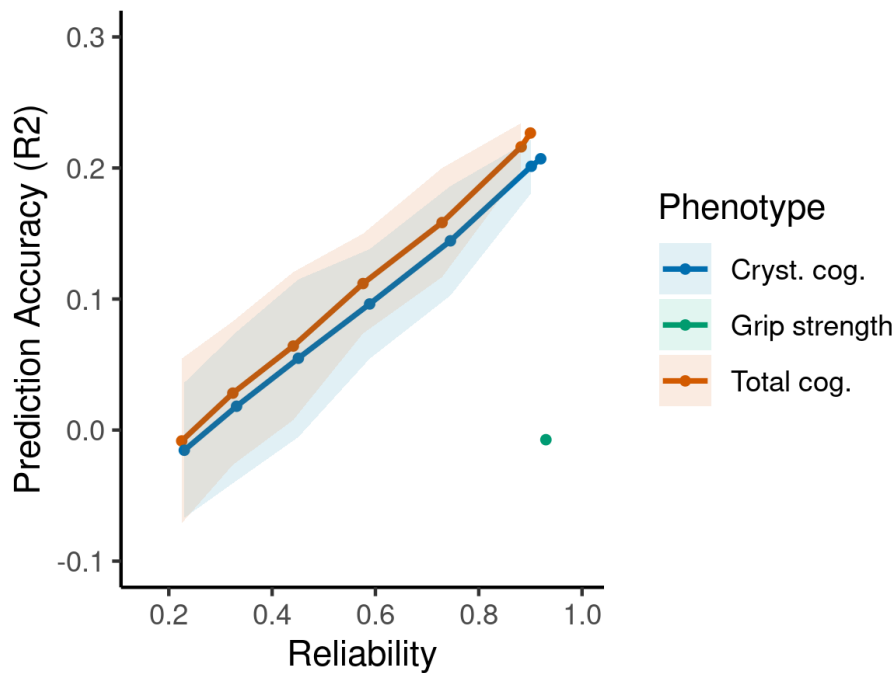


Supplementary Figure 5. Influence of feature reliability (functional connectivity) on the prediction of age with decreasing reliability. The x-axis represents the reliability of age, starting with empirically measured age at ICC ≈ 1.0 , followed by age with reduced reliability through simulations as in the main text. Feature reliability (represented by colours) was manipulated by reducing the amount of rsfMRI time course used to calculate functional connectivity, from the average of all four sessions collected on both days used in all main analyses to an average of 13 minutes collected on the first day only and finally, connectivity calculated from a single 6 minutes session collected on the first day in the anterior-to-posterior direction (same as only session in the UKB). Solid lines represent the mean prediction accuracy across all 100 simulated datasets in each reliability band, shaded areas represent 2 standard deviations in prediction accuracies.



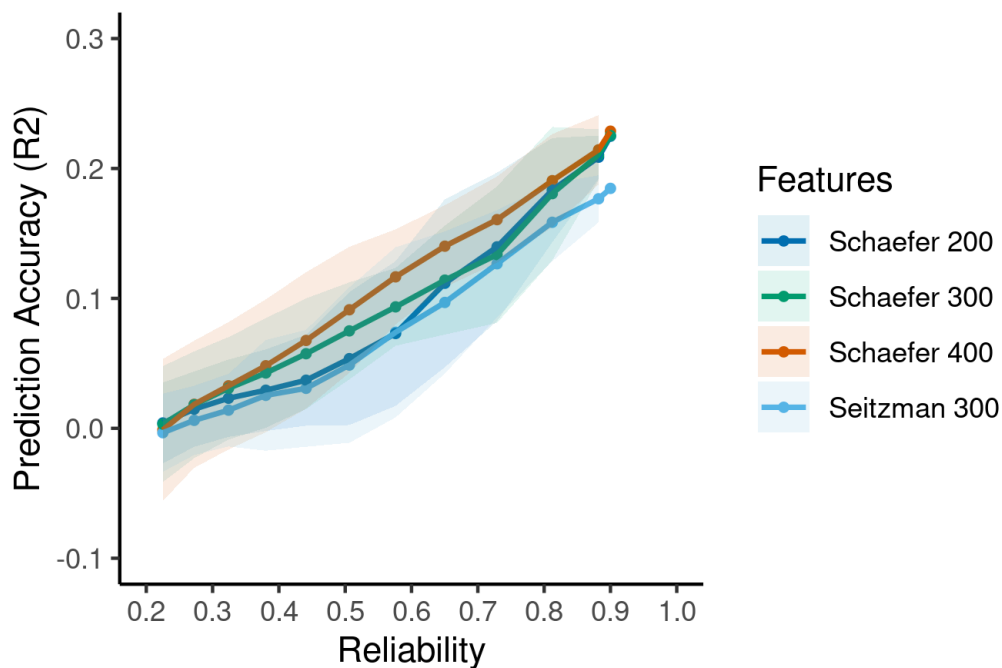
Supplementary Figure 6. Influence of feature reliability (functional connectivity) on the prediction of age with decreasing reliability. The x-axis represents the reliability of age, starting with empirically measured age at ICC ≈ 1.0 , followed by age with reduced reliability through simulations as in the main text. Age prediction from functional connectivity was calculated on day 1 and 2 rsfMRI acquisition separately. Both days had 13 minutes and 22 seconds of data. Solid lines represent the mean prediction accuracy across all 100 simulated datasets in each reliability band, shaded areas represent 2 standard deviations in prediction accuracies.

Sensitivity analyses - prediction of behaviour

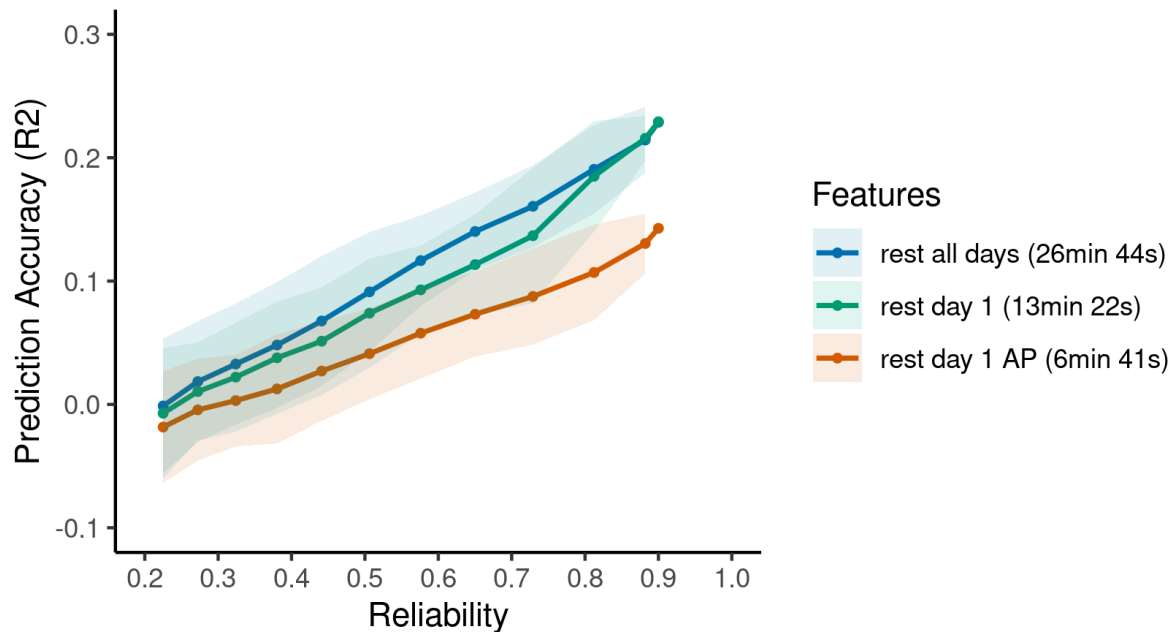


Supplementary Figure 7. Prediction of selected phenotypes with feature-wise confound (age, sex) regression. Grip strength could not be predicted when confounds were regressed. Solid lines represent the mean prediction accuracy across all 100 simulated datasets in each reliability band, shaded areas represent 2 standard deviations in prediction accuracies.

Sensitivity analyses - Total cognition

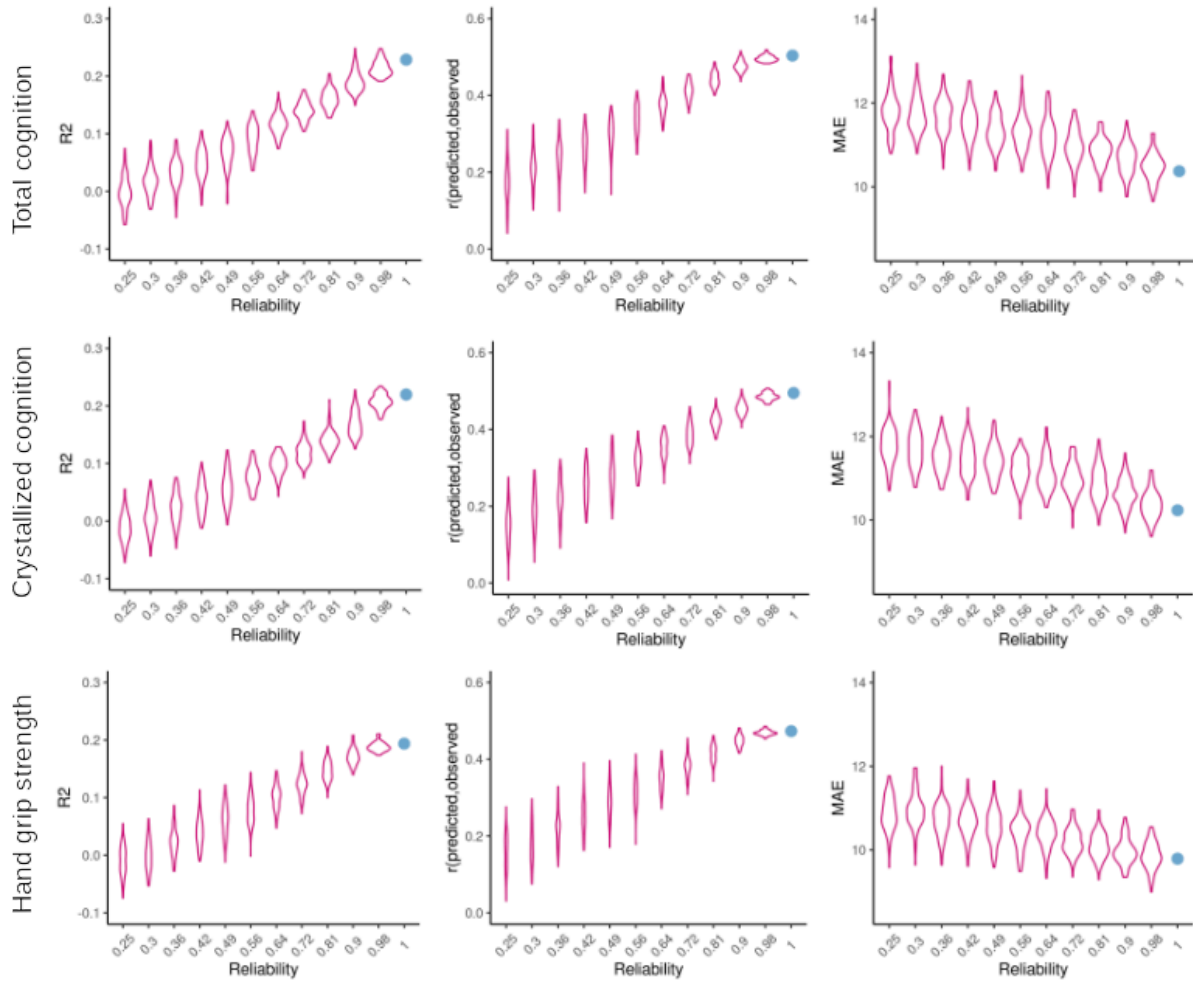


Supplementary Figure 8. Influence of feature granularity on prediction of total cognition with decreasing reliability. Solid lines represent the mean prediction accuracy across all 100 simulated datasets in each reliability band, shaded areas represent 2 standard deviations in prediction accuracies.



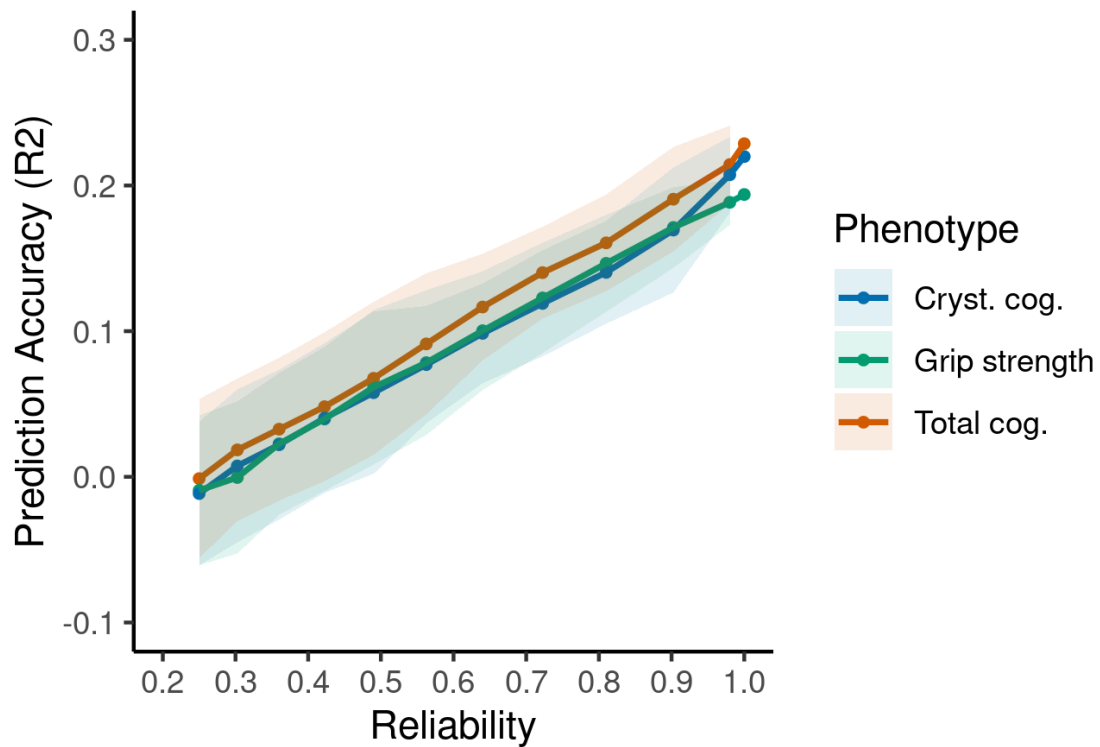
Supplementary Figure 9. Influence of feature reliability (functional connectivity) on prediction of total cognition with decreasing reliability. The x-axis represents the reliability of the NIH Toolbox total cognition composite score, starting at ICC = 0.9 based on Heaton et al. (2014), followed by total cognition with reduced reliability through simulations as in the main text. Feature reliability (represented by colours) was manipulated by reducing the amount of rsfMRI time course used to calculate functional connectivity, from the average of all four sessions collected on both days used in all main analyses to an average of 13 minutes collected on the first day only and finally, connectivity calculated from a single 6-minute session collected on the first day in the anterior-to-posterior direction (same as only session in the UKB). Solid lines represent the mean prediction accuracy across all 100 simulated datasets in each reliability band, shaded areas represent 2 standard deviations in prediction accuracies.

Phenotype prediction supplementary figures



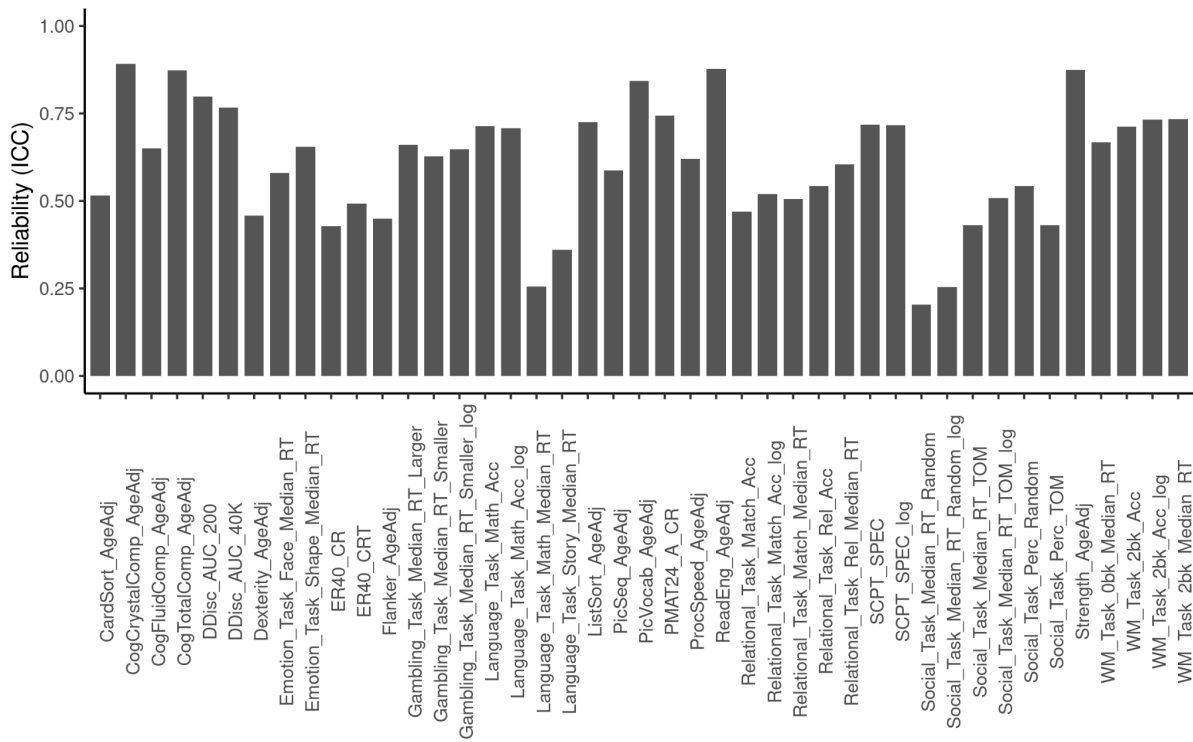
Supplementary Figure 10. R2, Mean absolute error (MAE) and correlation between observed and predicted targets for each target behaviours separately. Each violin plot summarises the accuracy of predicting 100 simulated datasets within each reliability band.

Uncorrected results for Figure 1



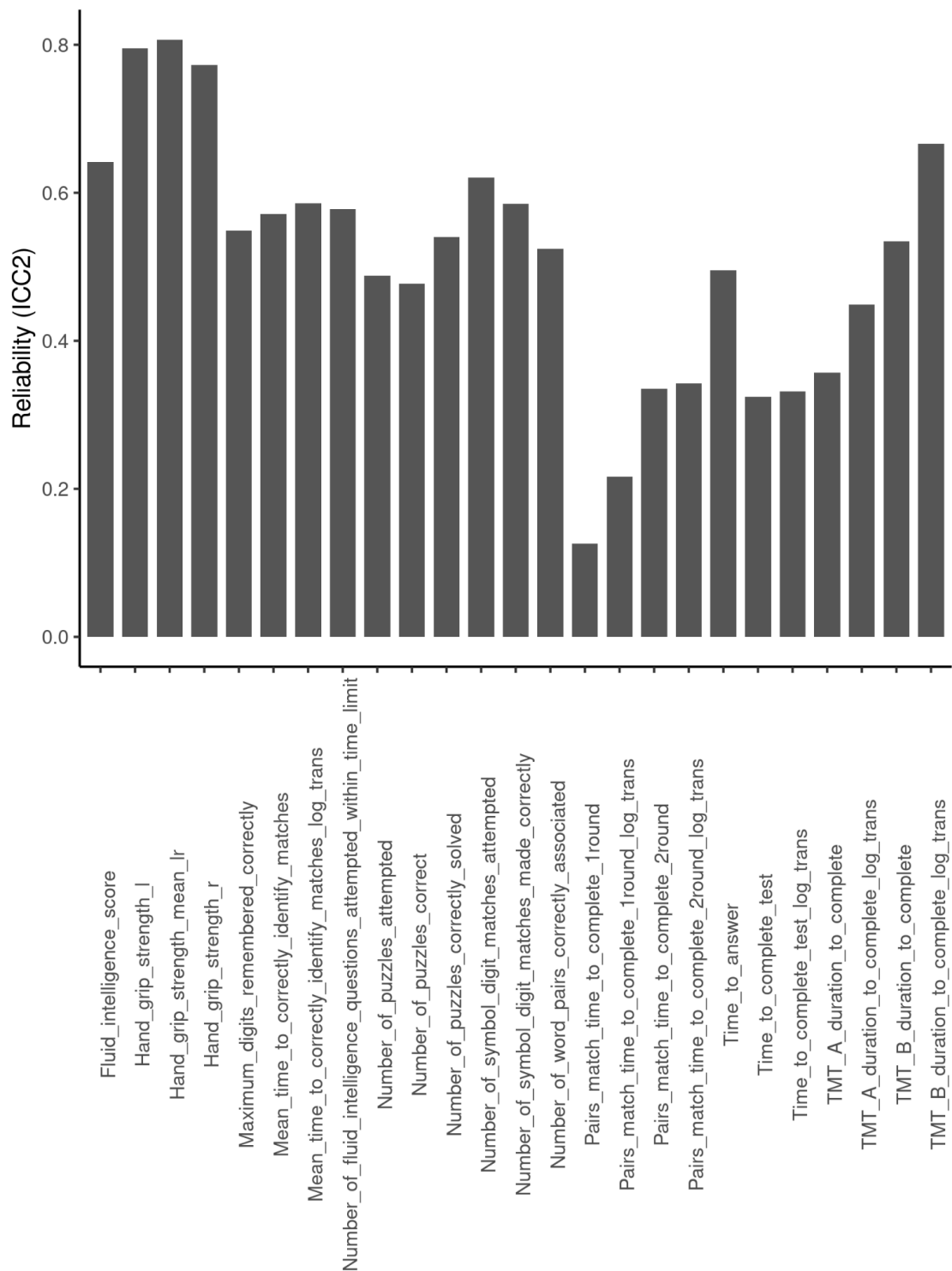
Supplementary Figure 11. Impact of reducing the correlation between original and simulated target scores (reflecting reduced reliability) on accuracy in prediction of total cognition composite score, crystallised cognition composite score and grip strength. Solid lines represent the mean across all 100 simulated datasets in each correlation band, shaded areas represent 2 standard deviations in prediction accuracies.

HCP young adult dataset predicted behaviours and respective reliability



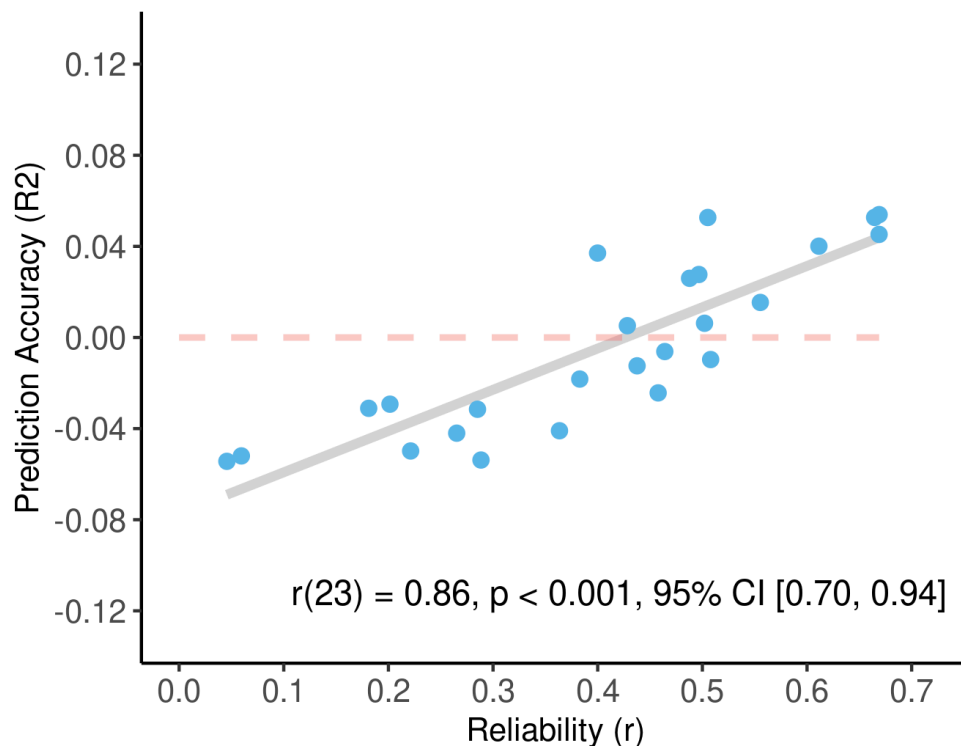
Supplementary Figure 12. Reliability of all behaviours predicted in the HCP-YA dataset

UKB predicted behaviours and respective reliability



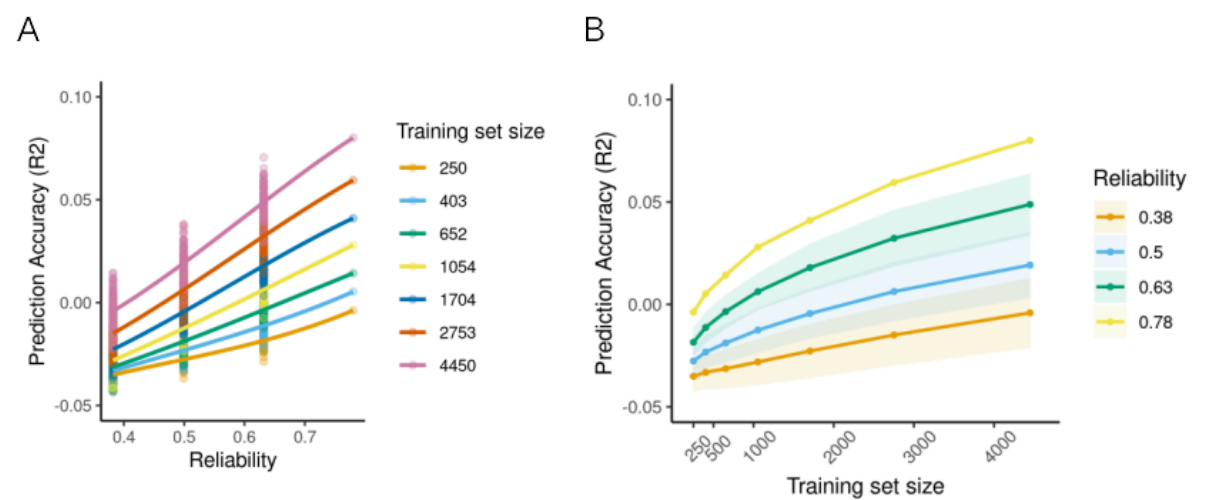
Supplementary Figure 13. Reliability of all behaviours predicted in the UKB dataset

Association between prediction accuracy and reliability in the ABCD dataset



Supplementary Figure 14. Association between reliability and prediction accuracy. Each data point represents one of 25 behavioural assessments in the ABCD. As measurements were collected from participants aged 9-10 at baseline and 11-12 at follow-up (mean retest interval = 23 months), reliability is calculated with test-retest (Pearson) correlation and not ICC. In developmental contexts, unlike ICC, correlation is robust to systematic age-related changes as it is not penalised by differences in means between baseline and follow-up data and different development rates across participants.

Prediction of cognitive flexibility measured trail-making task in UKB



Supplementary Figure 15. Prediction and subsampling in UKB. (A) Impact of training set size on original and simulated cognitive flexibility with reduced reliability. Panel (B) Impact of training set size on prediction accuracy in empirical and simulated data with varying levels of reliability. Solid lines represent the mean across all 100 simulated datasets in each correlation band and shaded areas represent 2 standard deviations in prediction accuracies. Results were fitted with an exponential function for illustration purposes and adjusted for the TMT task's reliability (ICC = 0.775) estimated in independent data by Fawns-Ritchie et al. (2020).

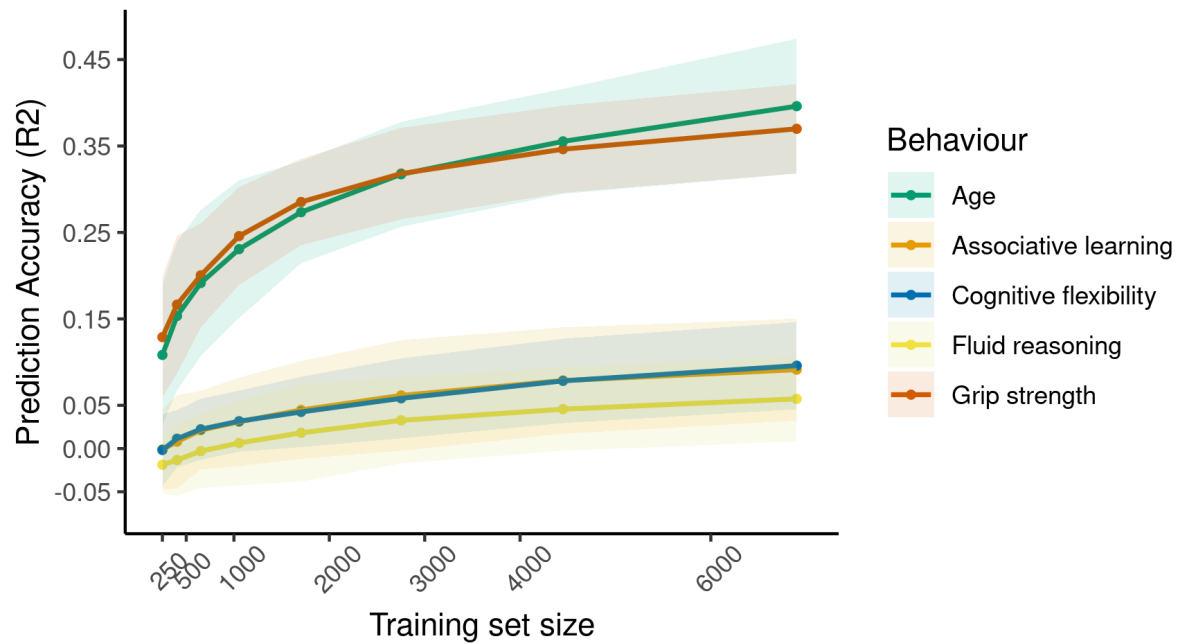
Learning curve results for empirical behaviours

Supplementary Table 1

Prediction accuracy (R2) of empirical behaviours across varying training set sizes

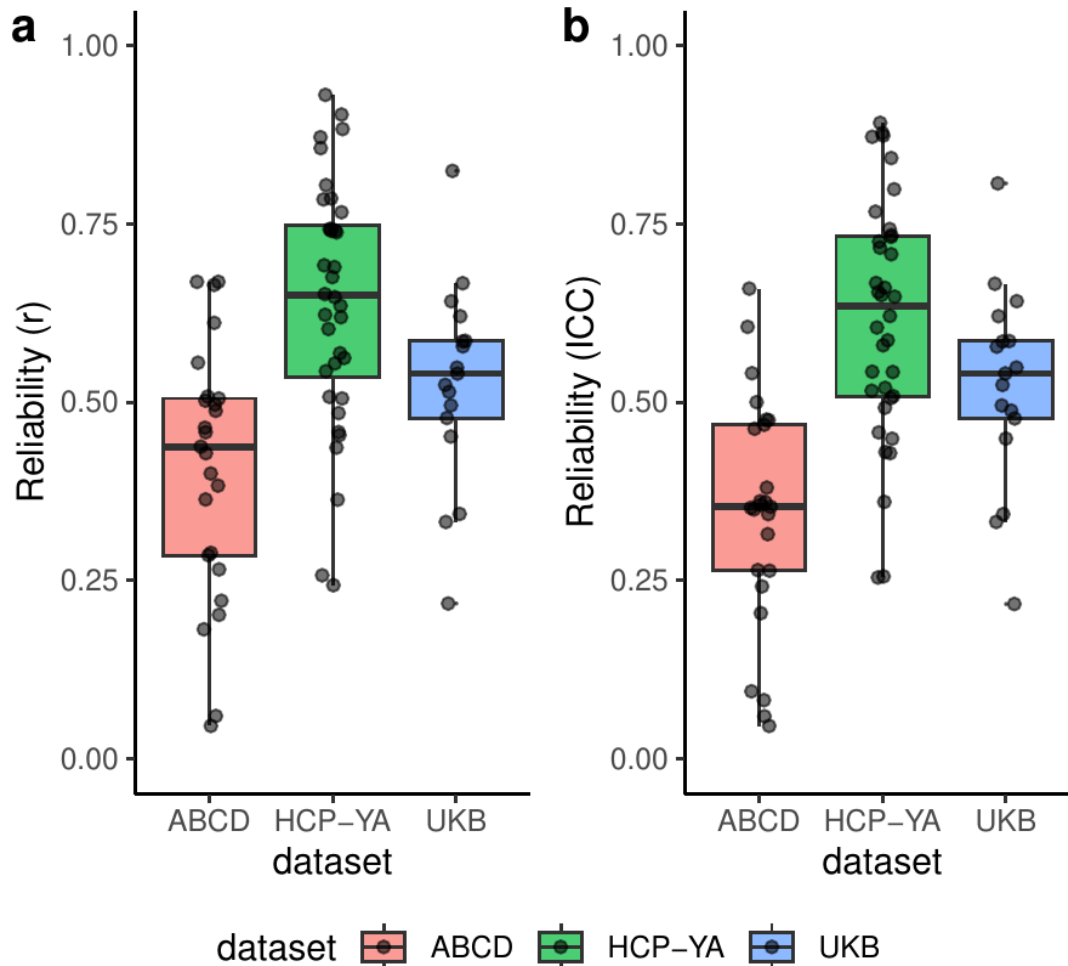
| Behaviour | Training Set Size | | | | | | |
|-------------------------------|-------------------|--------|--------|-------|-------|-------|-------|
| | 250 | 403 | 652 | 1054 | 1704 | 2753 | 4450 |
| Fluid Intelligence | -0.02 | -0.014 | -0.006 | 0.004 | 0.008 | 0.018 | 0.029 |
| Associative Learning (SDST) | -0.001 | 0.009 | 0.02 | 0.033 | 0.043 | 0.056 | 0.068 |
| Cognitive Flexibility (TMT B) | -0.002 | 0.007 | 0.0198 | 0.03 | 0.042 | 0.056 | 0.069 |
| Hand Grip Strength (mean) | 0.127 | 0.16 | 0.197 | 0.24 | 0.279 | 0.313 | 0.344 |
| Age | 0.107 | 0.149 | 0.189 | 0.228 | 0.272 | 0.316 | 0.354 |

Improvement in prediction accuracy with increased training set size



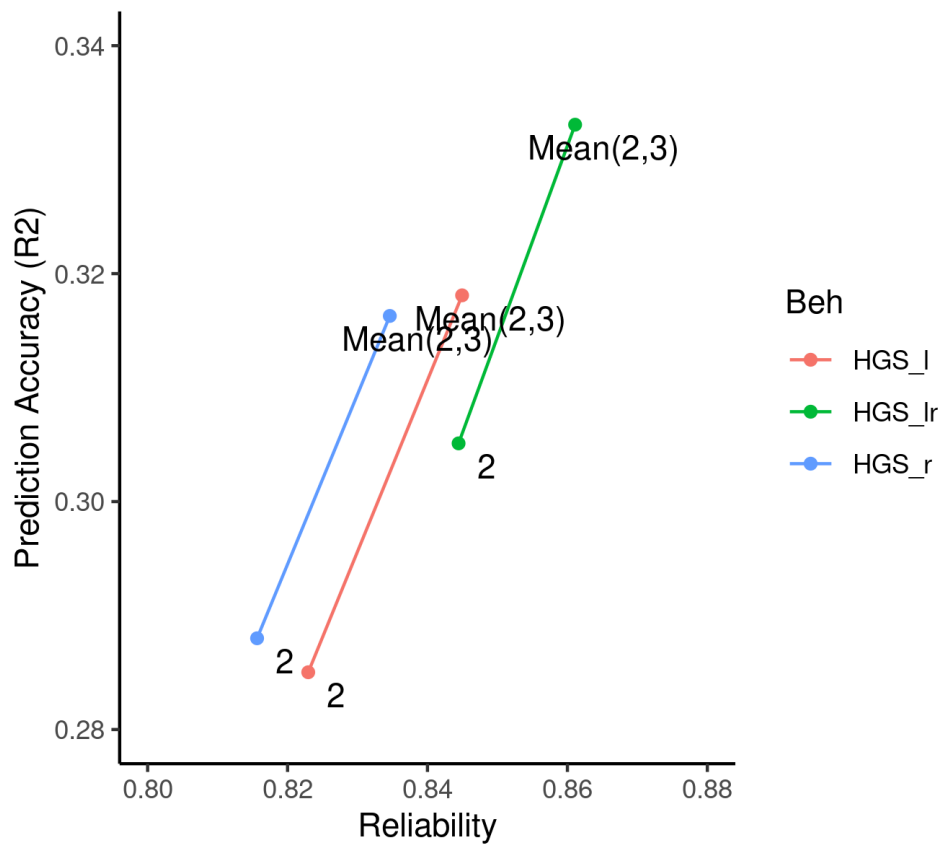
Supplementary Figure 16. Impact of training set size on prediction accuracy of empirical behaviours. Solid lines represent the mean accuracy across 100 subsamples and shaded areas represent 2 standard deviations in prediction accuracy. Abbreviations: SDST, Symbol Digit Substitution Test; TMT-B, Trail making task part B.

Distribution of test-retest correlations across HCP-YA, UK and ABCD datasets



Supplementary Figure 17. Boxplots of test-retest correlations (A) and ICC (B) of all measures used for assessing the association between prediction accuracy and reliability in Figure 2 of the main text. Overall median for test-retest correlations = 0.55; and ICC = 0.51. Both retest correlations and ICC are displayed as for some datasets, such as the ABCD, test-retest correlations may be more appropriate as systematic error coming from different rates of development across participants is not penalised.

Improvement in reliability and prediction accuracy with averaging across repeated assessments in grip strength



Supplementary Figure 18. Impact of increasing reliability by averaging in UKB hand grip strength prediction. Numbers denote UKB time points. Neuroimaging was collected at time point 2. Grip strength was averaged over time points 2 (neuroimaging baseline) and 3 (neuroimaging follow-up) to maximise the number of subjects. Reliability was calculated as Pearson test-retest correlation between time point 0 (baseline) and time point 2 as well as the average of 2 and 3. HGS_lr stands for the average of measurement over left and right hands. Abbreviations; HGS: Hand grip strength.

Supplementary methods

Comparison of acquisition and preprocessing parameters across datasets

Supplementary Table 2

Acquisition and preprocessing of datasets

| Parameter | Dataset | | |
|--------------------------------|--|--|---------------------------------------|
| | HCP-A | HCP-YA | UKB |
| Scanner | Siemens Prisma 3T | Siemens 'Connectom Skyra' 3T | Siemens Skyra 3T |
| Resting-state sessions | 4 runs across 2 days with AP and PA phase encoding on each day | 4 runs across 2 days with LR and RL phase encoding on each day | a single run acquired in AP direction |
| acquisition time | 488 frames per run (26 min total) | 1200 frames per run (58 min total) | 490 volumes (6 min) |
| TR/TE | 800/37 ms | 720/33 ms | 735/39 ms |
| Acquisition sites | 4 | 1 | 4 |
| gradient distortion correction | yes | yes | yes |
| intensity normalisation | yes | yes | yes |
| motion correction | yes | yes | yes |
| normalisation to MNI | yes | yes | yes |
| artefact removal | ICA-FIX | ICA-FIX | ICA-FIX |
| temporal filtering | bandpass filtered at 0.01 – 0.1 Hz | bandpass filtered at 0.01 – 0.1 Hz | highpass filtering |
| denoising | WM+CSF+GS regression | WM+CSF+GS regression | no |

Abbreviations; AP: anterior-to-posterior; PA: posterior-to-anterior; LR: left-to-right; RL right-to-left all refer to phase encoding directions

The exact sample size for predicted behaviours in HCP-A

Supplementary Table 3

Description of sample for behavioural prediction in HCP A

| Behaviour | Sample (Female) | Ages |
|---------------------------------------|-----------------|-------|
| Age (in months) | 647 (351) | 36-86 |
| Total cognition (age-adjusted) | 550 (308) | 36-86 |
| Crystallised cognition (age-adjusted) | 549 (308) | 36-86 |
| Hand grip strength (dominant hand) | 551 (306) | 36-86 |

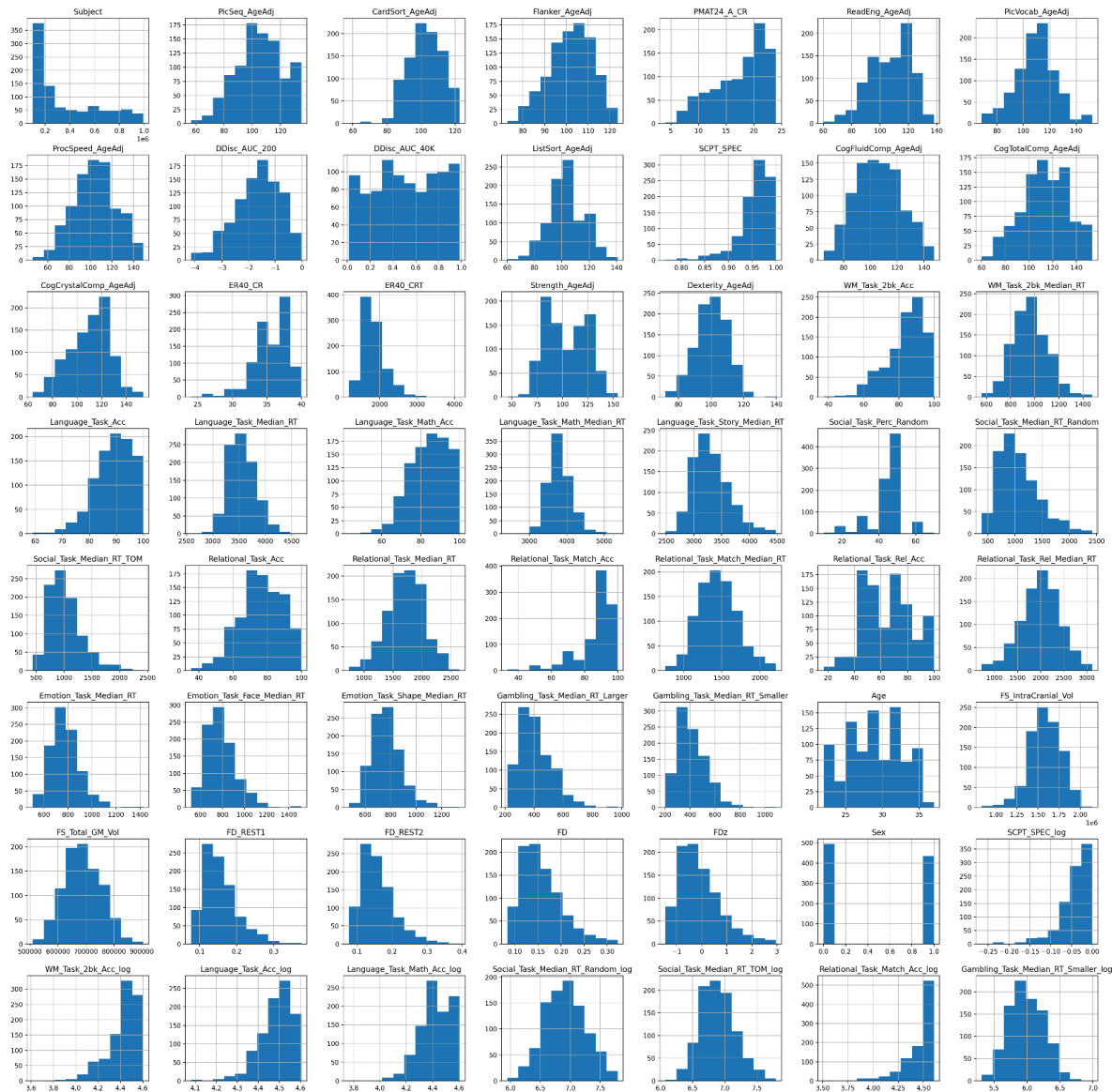
Behaviours selected for prediction in HCP-YA dataset

Supplementary Table 4

Predicted behaviours in HCP-YA

| Behaviour |
|------------------|
| PicSeq_AgeAdj |
| CardSort_AgeAdj |
| Flanker_AgeAdj |
| PMAT24_A_CR |
| ReadEng_AgeAdj |
| PicVocab_AgeAdj |
| ProcSpeed_AgeAdj |
| DDisc_AUC_200 |
| DDisc_AUC_40K |
| ListSort_AgeAdj |
| SCPT_SPEC |

CogFluidComp_AgeAdj
CogTotalComp_AgeAdj
CogCrystalComp_AgeAdj
ER40_CR
ER40_CRT
Strength_AgeAdj
Dexterity_AgeAdj
WM_Task_2bk_Acc
WM_Task_2bk_Median_RT
WM_Task_0bk_Median_RT
Language_Task_Math_Acc
Language_Task_Math_Median_RT
Language_Task_Story_Median_RT
Social_Task_Perc_Random
Social_Task_Perc_TOM
Social_Task_Median_RT_Random
Social_Task_Median_RT_TOM
Relational_Task_Match_Acc
Relational_Task_Match_Median_RT
Relational_Task_Rel_Acc
Relational_Task_Rel_Median_RT
Emotion_Task_Face_Median_RT
Emotion_Task_Shape_Median_RT
Gambling_Task_Median_RT_Larger
Gambling_Task_Median_RT_Smaller



Supplementary Figure 19. Distribution of all predicted behaviours HCP-YA

Excluded fields for UKB sample

This section details excluded and included fields when parsing UKB subjects. Subjects with a history of neurological disease, as reported in (Kweon et al., 2022) and additionally subjects with sleep apnoea were excluded.

Supplementary Table 5

Excluded fields in UKB participants

| | |
|---|---|
| Excluded ICD codes: | 'G473', 'F00', 'F01', 'F02', 'F03', 'G30', 'G20', , 'G21', 'G23', 'G31', 'G32', 'G610', 'G35', , 'G37', 'I63', 'G463', 'G464', 'I64', 'I694', , 'C70', 'C71', 'D33', 'I60', 'I61', 'I62', 'I691', , 'I692', 'I693', 'G060', 'G07', 'I671', 'Q282', , 'Q283', 'G80', 'A521', 'A504', 'I64', 'A83', , 'A86', 'B011', 'B020', 'B262', 'A85', 'B004', , 'B582', 'A84', 'B050', 'B941', 'G04', 'A321', , 'G05', 'G40', 'F803', 'S07', 'T040', 'A80', , 'A81', 'A82', 'A83', 'A84', 'A85', 'A86', 'A87', , 'A88', 'A89', 'G45', 'C70', 'C793', 'D32', , 'D33', 'G03', 'A170', 'A171', 'A203', 'G01', , 'G02', 'G00', 'G07', 'G122', 'Q05', 'Q760', , 'P100', 'I60', 'S066', 'P103', 'G45', 'F' |
| Self-reported illness code (Data-Coding 6): | 1123, 1263, 1262, 1258, 1256, 1261, 1397, 1081, 1032, 1491, 1245, 1425, 1433, 1246, 1264, 1266, 1244, 1583, 1031, 1659, 1247, 1259, 1240, 1524, 1083, 1086, 1082 |

Behaviours selected for prediction in UKB dataset

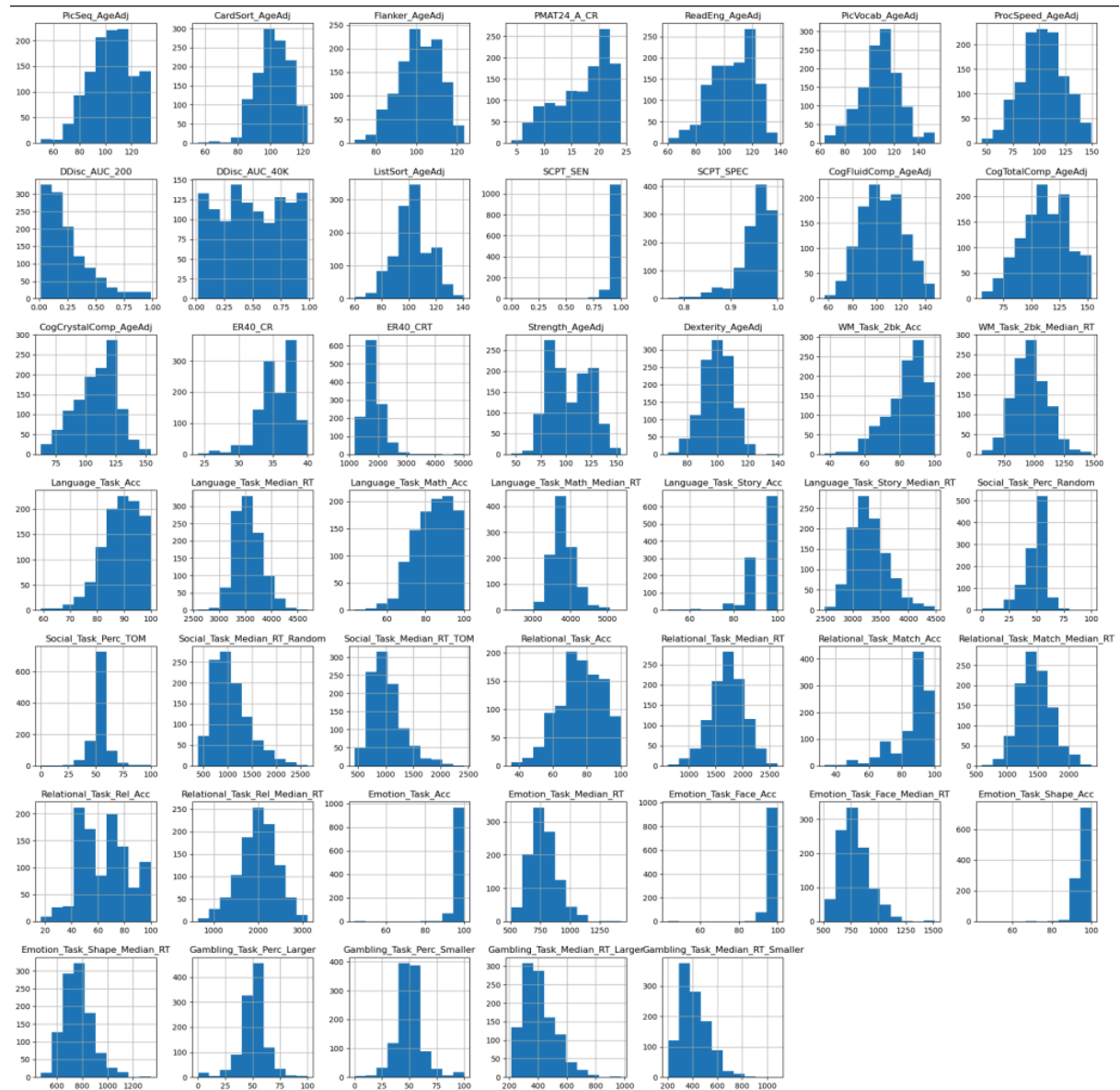
Supplementary Table 6

Predicted behaviours in UKB

| Behaviour | Data-field |
|--|------------|
| Pairs_match_time_to_complete_1st_round-2.0 | 400 |
| Pairs_match_time_to_complete_2nd_round-2.0 | 400 |
| Maximum_digits_remembered_correctly-2.0 | 4282 |
| Time_to_complete_test-2.0 | 4285 |
| Time_to_answer-2.0 | 4288 |
| TMT_A_duration_to_complete-2.0 | 6348 |

| | |
|--|--------|
| TMT_B_duration_to_complete-2.0 | 6350 |
| Number_of_puzzles_correctly_solved-2.0 | 21004 |
| Number_of_puzzles_attempted-2.0 | 6383 |
| Fluid_intelligence_score-2.0 | 20016 |
| Mean_time_to_correctly_identify_matches-2.0 | 20023 |
| Number_of_fluid_intelligence_questions_attempted_within_time_limit-2.0 | 20128 |
| Number_of_word_pairs_correctly_associated-2.0 | 20197 |
| Number_of_puzzles_correct-2.0 | 6373 |
| Number_of_symbol_digit_matches_attempted-2.0 | 23323 |
| Number_of_symbol_digit_matches_made_correctly-2.0 | 23324 |
| Hand_grip_strength_mean_lr-2.0* | 46, 47 |

*Average of Hand_grip_strength_l-2.0 and Hand_grip_strength_r-2.0



Supplementary Figure 20. Distribution of all predicted behaviours in UKB

Behaviours selected for prediction in ABCD

Supplementary Table 7

Predicted behaviours in ABCD

Behaviour

nihtbx_picvocab_fc

nihtbx_flanker_fc

nihtbx_pattern_fc
nihtbx_picture_fc
nihtbx_reading_fc
nihtbx_cryst_fc
pea_ravlt_sd_trial_vi_tc
pea_ravlt_ld_trial_vii_tc
lmt_scr_perc_correct
lmt_scr_perc_wrong
lmt_scr_avg_rt
lmt_scr_rt_correct
tfmri_mid_all_beh_srwpfb_nt
tfmri_mid_all_beh_lrwpfb_mrt
tfmri_mid_all_beh_srwpfb_mrt
tfmri_mid_all_beh_lrwpfb_nt
tfmri_sst_all_beh_total_mssrt
tfmri_nb_all_beh_c2b_rate
tfmri_nb_all_beh_c2b_mrt
tfmri_nb_all_beh_c0b_rate
tfmri_nb_all_beh_c0b_mrt
tfmri_rec_all_beh_place_dp
tfmri_rec_all_beh_negf_dp
tfmri_rec_all_beh_neutf_dp
tfmri_rec_all_beh_posf_dpr

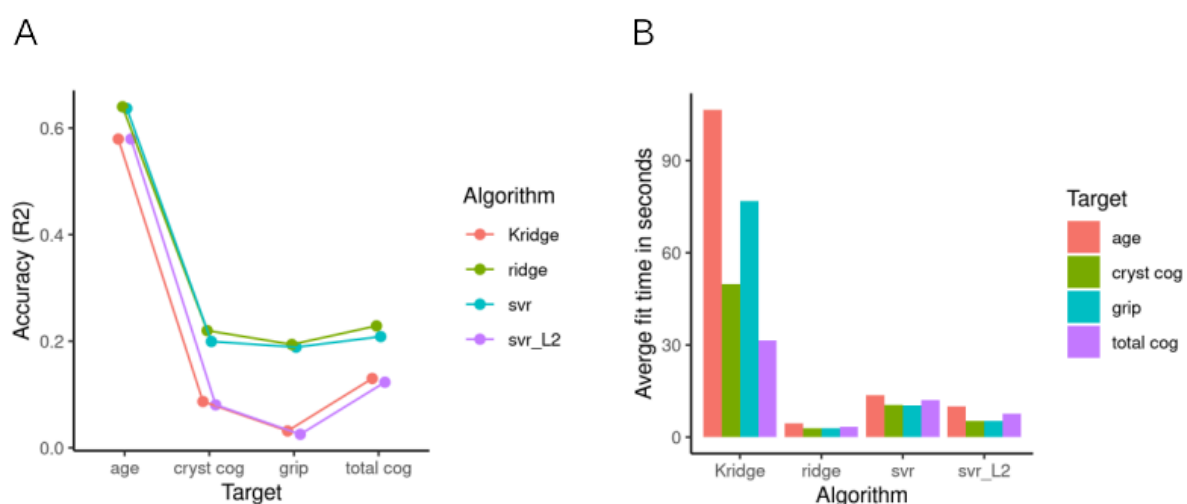
Comparison of accuracy to computation time

Given the large number of predictions that were necessary to conduct for our simulation analyses, we first tested algorithms commonly used in the literature (Supplementary Figure

3) to find the best computation time to accuracy trade-off (measured with R2). This was not meant as an exhaustive comparison to identify the perfect pipeline. Four algorithms were tested: linear ridge regression, kernel ridge regression and two flavours of support vector regression all implemented in the Scikit learn library [version 0.24.2, (Pedregosa et al., 2011)]. A 10-fold cross-validation scheme was used to evaluate the performance of all models. Hyperparameter optimisation of the alpha regularisation parameter for ridge regression and kernel ridge regression was performed using a nested cross-validation scheme (5-fold cross-validation for kernel ridge and leave-one-out cross-validation for ridge regression) embedded with the 10-fold cross-validation. Next, two implementations of linear support vector regression were tested (sklearn.svm.LinearSVR with squared epsilon-insensitive (L2) loss function and sklearn.svm.SVR; see https://github.com/MartinGell/Prediction_Reliability for details). A heuristic was used to efficiently calculate the hyperparameter C (Helleputte, Paul, & Gramme, 2021):

$$c = \frac{1}{\frac{1}{n} \sum_{i=1}^n \sqrt{G[i,i]}}$$
 where G = matrix multiplication of features and transpose of features (here functional connectivity).

Prior to training, subjects with behavioural data over $\pm 3SD$ were removed and neuroimaging features were z-scored within participants (average connectomes from HCP dataset were first transformed back to r values from Fisher-z scores) to keep features consistent across algorithms as this step was required for kernel ridge regression. Within each training fold, neuroimaging features were z-scored across participants before models were trained (using Sklearn's `pipeline`).



Supplementary Figure 21. Comparison of algorithms. (A) Displays prediction accuracy (R2) for all behaviours of interest predicted using different algorithms: Kridge = Kernel ridge regression, ridge = Linear ridge regression, svr = Support vector regression and svr_L2 =

support vector regression. (B) Displays the average training time of a single mode across cross-validation for all tested behaviours and algorithms.

References

Helleputte, T., Paul, J., & Gramme, P. (2021). *LiblineaR*. Retrieved from

<https://search.r-project.org/CRAN/refmans/LiblineaR/html/heuristicC.html>

Kweon, H., Aydogan, G., Dagher, A., Bzdok, D., Ruff, C. C., Nave, G., ... Koellinger, P. D.

(2022). Human brain anatomy reflects separable genetic and environmental

components of socioeconomic status. *Science Advances*, 8(20), eabm2923. doi:

10.1126/sciadv.abm2923

Pedregosa, F., Varoquaux, G., Gramfort, A., Michel, V., Thirion, B., Grisel, O., ... Duchesnay,

É. (2011). Scikit-learn: Machine Learning in Python. *The Journal of Machine Learning*

Research, 12(null), 2825–2830.